ИНСТИТУТ ЯДЕРНОЙ ФИЗИКИ
им. Г.И. Будкера СО РАН

А.Д. Букин, А.А. Михайличенко

ОПТИМАЛЬНЫЙ ВЫБОР МИШЕНИ ДЛЯ ПОЛУЧЕНИЯ ПОЛЯРИЗОВАННЫХ e^+e^- ДЛЯ ЛИНЕЙНОГО КОЛЛАЙДЕРА

ИЯФ 92-76

НОВОСИБИРСК

OPTIMIZED TARGET STRATEGY FOR POLARIZED ELECTRONS AND POSITRONS PRODUCTION FOR LINEAR COLLIDER

A.D.BUKIN, A.A.MIKHAILICHENKO

G.I.Budker Institute of Nuclear Physics
630090, Novosibirsk, Russia

ABSTRACTS

For polarized particles generation with the help of radiation from helical wiggler, applicable in Linear Collider, new calculations are represented. This calculations are made with the codes UNIMOD2, CONVER and OBRA, concerning the choice of optimal thickness and form of the target for different energy of initial beam. Optimized target gives maximal yield of polarized particles. Heating conditions of the target are described also.

Estimations were made also how to test this method of particle production at SLAC Linac.

ОПТИМАЛЬНЫЙ ВЫБОР МИШЕНИ ДЛЯ ПОЛУЧЕНИЯ ПОЛЯРИЗОВАННЫХ ЭЛЕКТРОНОВ И ПОЗИТРОНОВ ДЛЯ ЛИНЕЙНОГО КОЛЛАЙДЕРА

А.Д.БУКИН, А.А. МИХАЙЛИЧЕНКО

Институт Ядерной Физики СО РАН им.Г.И.Будкера
630090, Новосибирск, Россия

Аннотация

Для метода получения поляризованных частиц для использования в Линейных коллайдерах с помощью излучения из спирального ондулятора, представлены новые вычисления по программам UNIMOD2, CONVER и OBRA, связанные с выбором оптимальной толщины и формы мишени для различного значения энергии первоначального пучка. Оптимизированая мишень обеспечивает максимальный выход поляризованных частиц. Рассмотрен тепловой режим работы мишени.

Сделаны также оценки для того, чтобы тестировать этот метод генерирования частиц на линейном ускорителе SLAC.

1.INTRODUCTION

The method for obtaining highly polarized electrons and positrons was described in [1-5]. In this method helical undulator is used for production of *circularly polarized photons*. After that these photons are converted into positrons and electrons in a *thin* target. At the top of energy spectrum the *longitudinally polarized particles* are produced. Not polarized particles can be used as initial ones and after their passing through undulator they are loosed only few percent of its energy without perturbing of transverse emittance.

Such correlation of polarization and energy makes possible to use simple procedure of separation of polarized particles. It is necessary to select particles with *highest energy*.

For polarized particles selection or, respectively, energy selection, there was discussed the RF cavity excited for deceleration of particles and, hence, providing some energy threshold [1], and combination of the short focusing Lithium lens and the diaphragm, which is the simplest energy separation system [2]. The lens provides a quarter wave transformation for the particles near the maximum of the energy. Additional advantage is that the Lithium lens [11] is focusing the only particles with necessary sign of charge in narrow energy interval and defocusing the particles of opposite sign of charge. This is useful, because a quantity of created particles with opposite sign of charge is approximately equal and distributed in wide energy interval down to the energy of the gamma-quanta, and such defocusing of not necessary particles prevents them to penetrate into the first accelerating structure and loading of it, initiating multipaction, sparking and heating.

It seems, that future Linear Colliders will operate at

repetition rate above 100 Hz, moreover, CLIC is planned to operate at 1.7 kHz. TESLA is planned to operate at 10 Hz, but about 0.8 millisecond of beam duty of 800 bunches. For this repetition rate, or duty factor, utilization of the Lithium lens becomes possible only with technology with liquid Lithium [16], cause of heating. From the other side, secondary particles provided by conversion system with the undulator are good forming in narrow angle peak, strongly limited of maximal energy, which makes possible to use for preliminary focusing the solenoidal *superconducting concentrator* with quadrupole matching triplet as following focusing device. This combination is not sensitive for repetition rate also. Final separation connected with scrapping the particles in the place with high level of dispersion, but low envelope function. Preliminary separation which goes with quads also makes possible to defocusing the particles of not necessary sign of charge. Here we briefly touch this possibility, planning to investigate it more carefully in other place.

For maximal efficiency, the photons of maximal energy are desirable. Difficulties of obtaining of the photons of maximal energy is connected with restrictions for usage of short period of the undulator, which is mostly defined by its aperture. The aperture of undulator is defined by the beam size and requirements of homogeneity of magnetic field in aperture. For fixed aperture, technical limitation occurs at the period of the order of aperture itself. Also important limitations comes from resistive wall instability, connected with finite conductivity of the material of the beam chamber of undulator [14]. Fortunately, the helical undulator with superconducting windings design [5], has cooled vacuum chamber, which provides an order of magnitude less level of specific resistance of inner surface.

Output polarization is a function of averaged polarization of created particles, which defined by its relative energy and polarization of gamma beam from undulator, which depends of the opening angle of the target irradiation. So, it is necessary to use diaphragm to prevent illumination of the target with photons with low level of polarization, which are radiated with the angle, bigger, than the angle $\theta > \theta^* = (1 + p_\perp^2)^{1/2}/\gamma/3$, where $p_\perp = eH_\perp\lambda_0/(2\pi m_0 c^2)$, λ_0 - is the period of the magnetic field, $H_\perp$ -

is the magnetic field strength on the axis of the undulator. Estimation of the radius of the diaphragm as a function of desirable averaged degree of polarization is represented lower, see page 12, and value of the radius is about 0.3 mm.

First results with numerical calculations were represented in [2]. The results, obtained here, confirm the output of the first publication [1] of possibility to convert the particles into polarized ones with the efficiency, more than unity, and polarization at least 65% . Here, as it was mentioned, used combination of the Lithium lens and diaphragm for separation of the particles over energy.

In this paper we briefly describe the codes UNIMOD2, CONVER [10,13] and new one - OBRA. This codes are working one after another (CONVER and OBRA are working in PC media), and with OBRA calculated all necessary parameters, including polarization of secondary beams at the *output of the target* with accuracy not less than 10% . The value of accuracy is limited only by the PC capacity of the files, prepared at big computer, and, in principle, can be higher, up to 1%. The code UNIMOD2 has a good agreement with experimental data and used for calculations of efficiency of registration of the particles in detectors. There is possible to use output parameters from the OBRA and CONVER code for following calculations of the further optics.

The conversion efficiency about 7 % per one photon of 40 MeV yields the necessity to generate about 15 photons by one initial particle in the energy interval about 10% around the maximal energy. For $p_\perp = 0.50$ and angle of separation $\theta < \theta^*/3 = (1+p_\perp^2)^{1/2}/3$, for providing this amount of the particles with the value of polarization of the photon beam about 99 % , it is necessary to have the number of periods in undulator about $2\ 10^4$ (see Table 4). For $\lambda_0 = 0.5$ cm this gives 100 meter of total length. The resulting degree of polarization of the positrons (or electrons) can achieve 80% .

Special calculations were made to obtain efficiency for different *profile* of the target. The general output is that the simple configuration of the target as a flat disc of the thickness about $0.5X_0$ is preferable from all aspects of the problem. Diameter of the illuminated surface on the disc defined by the

diameter of the diaphragm.

Utilization of PC in calculation makes it more convenient and operative. Herewith we did not try to represent finished conversion scheme for Linear Collider, but demonstrate the *possibilities* of the codes.

Let us begin its brief description.

2. INTERACTION OF THE GAMMA-QUANTA WITH MATTER.

Here we remind, briefly, some formulas for interaction of the gammas with the matter, which makes understanding easy. Accurate analytical formulas used in simulations are collected in [18]. The differential cross-section of pair production is [12]:

$$\frac{d\sigma(E_\gamma,E_+)}{dE_+} \cong 4\,\frac{Z^2\,\alpha\,r_0^2}{E_\gamma-2m_0c^2}\,ln(183/Z^{1/3})G\left(\frac{E_+}{E_\gamma}\right) \cong \frac{A}{N_0}G\left(\frac{E_+}{E_\gamma}\right)\frac{1}{(X_0E_\gamma)}$$

where the following conditions are supposed: $E_\gamma,\ E_\pm \gg m_0,\ \frac{2E_+E_-}{m_0E_\gamma} \gg \frac{137}{Z^{1/3}}$ (total screening). Symmetrical function G(x) (with respect to the point x = 0.5) is equal to

$$G(x) = x^2+(1-x)^2+\frac{2}{3}\,x\cdot(1-x) - \frac{x\cdot(1-x)}{9\cdot ln(183\cdot Z^{-1/3})},$$

E_γ is the photon energy, E_+ and E_- are the total energies of the produced positron and electron, energy conservation law gives the relation $E_-= E_\gamma- E_+$, Z and A are the atomic number and weight, $r_0=e^2/m_0c^2$, $N_0= 6.022\cdot10^{23}$ is Avogadro number, radiation length X_0 is defined by

$$X_0^{-1} \cong 4\,r_0^2\,\alpha\,\frac{N_0}{A}\,Z^2\,ln(183/Z^{1/3})\ [cm^2/g]$$

The total cross-section of the pair production per nucleus in case of full screening is [12]

$$\sigma_{pair} \cong 4\,Z^2\alpha\,r_0^2\cdot\left(\frac{7}{9}\,ln(183/Z^{1/3})-\frac{1}{54}\right) \cong \frac{7}{9}\cdot\frac{A}{N_0}\cdot\frac{1}{X_0}$$

So, the expression for differential cross-section becomes

$$\frac{d\sigma(E_\gamma,E_+)}{dE_+} \cong \sigma_{pair}\cdot\frac{G(E_+/E_\gamma)}{E_\gamma}$$

for ultrarelativistic energy and total screening.

Total number of produced positrons by incident photons in all energy spectrum by a target of relative thickness $dt/X_0 \Rightarrow d\tau$ is

$$dN_+ \cong \frac{7}{9}\,N_\gamma\cdot d\tau\ ,$$

where N_γ is the number of incident photons.

For calculation of the yield of the positrons it must be taken into account that the number of photons decreases exponentially

$$N_\gamma= N_\gamma^0\ exp(-\tfrac{7}{9}\tau)\ ,\quad dN_+(\tau,d\tau) \cong N_\gamma^0\cdot exp(-\tfrac{7}{9}\tau)\cdot d\tau$$

In the energy region of interest E_γ= 20÷30 MeV the relation between cross-section of Compton effect and cross-section of the pair production is [5]

$$\frac{\sigma_{Compton}}{\sigma_{pair}} \approx \frac{\pi m_0\cdot[ln(2E_\gamma/m_0)+\frac{1}{2}]}{4\alpha ZE_\gamma\cdot(\frac{7}{9}\,ln\frac{183}{Z^{1/3}}-\frac{1}{54})} \approx 4\div6\%,$$

where Z = 74 of Tungsten was used. For Titanium target (see page 20) this ratio increase in 74/22 ≅ 3.3 times up to 15÷20 %.

Formula for the spectrum of created positrons can be written as follows

$$\frac{d^2N_+}{dE_+d\tau} = \int_{E_+^{min}}^{E_+^{max}}\frac{dN_\gamma}{dE_\gamma}\cdot\frac{d\sigma(E_\gamma,E_+)}{dE_+}\,dE_\gamma,$$

where $E_+^{max} = E_\gamma^{max}- 2m_0c^2$, determined by the photon source, E_+^{min} is the minimal value of collected energy, and the expression dN_γ/dE_γ for spectrum of the incident photons must be substituted for the gammas, produced in helical undulator [6,17].

For the full utilization of gammas, the target of maximal thickness must be taken. But all this contradicts the requirements of minimizing energy and angular dispersion. So, the choice of the thickness is the subject of optimization. Other circumstance which

must be taken into account is nonlinear dependence of the fractional losses of the energy by the particle as a function of the thickness. So, for purpose of lowering the heating of the target it is preferable to take the thickness of the target *less*, that optimized one, as it can be seen from Tables 5-11. For example, lowering the thickness of the Tungsten target from 0.1 cm to 0.02 cm decrease the conversion efficiency for Gammas of 10 MeV from 1.1% to 0.5% (Table 13), but the fractional losses decrease about 50 times. For compensation of this decrease of efficiency, *few targets* can be installed serially, see Chapter 5.

The optimal thickness, as it will be shown lower, is about $\tau \cong 0.5[X_0]$ and depends of the energy of gammas. Notice here, that the *effective* thickness in this case is less than $\tau/2$, which is connected with the process of absorption and diffusion of the particles in material of the target: *not all* particles, which created in the media, will reach the end of the target and will be collected in definite angle. Extreme example gives thick target, where it is evident, that the only particles from the end parts, according to absolute possible energy losses can reach the border of the target. This process dominates when energy of gammas decreases. This calculations goes in OBRA code numerically, cause the longitudinal distance of the point where the particle created also exists in output file of CONVER code.

In [15] there is proposed ceramic target and Titanium one. From previous formulas it can be seen, that the number of created particles for the target of thickness t depends in combination $\delta = t/l_{X0}$, and formally the same ratio δ gives the same yield of positrons. The reason for usage of light materials -the bigger heat capacity due to Dulong-Petite law. The efficiency of the conversion, calculated for Titanium target with our codes are represented in Table 13. Here it is necessary to take into account the ionization losses. Critical Energy, for which ionization losses become equal to radiation losses defined by well known relation $E_{cr} \cong 600/Z$ [MeV], and for fixed energy of the quanta, ionization losses are dominate for material with low value of Z.

3. POLARIZATION.

As it was mentioned, the resulting polarization of the created beam (e^+ or e^-) is the function of fractional interval of collected energy and mean polarization of the photon beam. In our calculations we used *integrated* characteristics for the photon beam, cause the mean level of polarization is very high, when the diaphragm is used - about 97% -and additional calculation with personal photons exceed the accuracy of calculations.

Longitudinal polarization of the created particle is a function of its energy E_+, E_- and polarization ξ_2 of gamma - quanta as it was shown in [7]

$$\vec{\zeta} = \xi_2 \cdot [f(E_+,E_-)\cdot\vec{n}_{\parallel} + g(E_+,E_-)\cdot\vec{n}_{\perp}\ ] = \vec{\zeta}_{\parallel} + \vec{\zeta}_{\perp},$$

where $\vec{n}_{\parallel}$ is directed along the initial direction of gamma radiation and $\vec{n}_{\perp}$ lies in the plane, rectangular to this direction. Represent here analytical expression for f [7]

$$f = E_{\gamma}\cdot\frac{E_+\psi_1 - E_-(\psi_1 - 2\cdot\psi_2/3)}{(E_+^2 + E_-^2)\psi_1 + 2\cdot E_+\cdot E_-\cdot\psi_2/3},$$

where

$$\psi_1 = ln(183\cdot Z^{-1/3}) - f(\alpha Z),\quad \psi_2 = \psi_1 - \tfrac{1}{6},\quad f(x) = x^2\sum_{n=1}^{\infty} 1/[n(n^2+x^2)].$$

For $E_+ \cong E_{\gamma}$, $f \cong 1$.

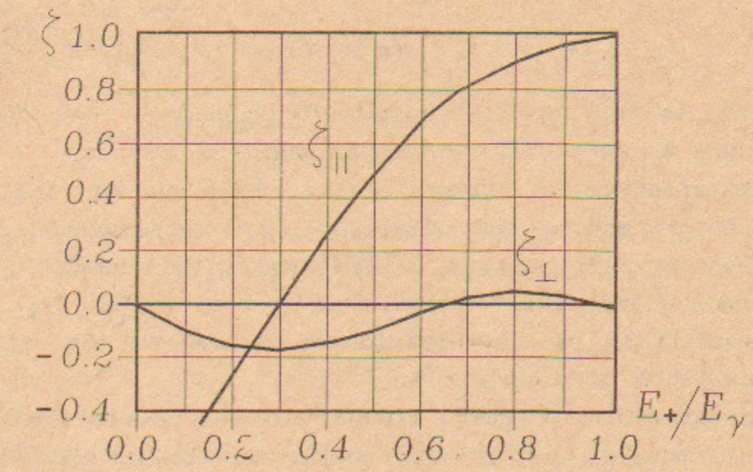

Fig.1. f and g as a functions of energy .

The view of the graph is practically independent of the photon energy. So it is necessary to select the energy of final particles near maximum of energy spectrum.

The mean level of polarization of created positrons or electrons is

$$\langle \zeta_{\parallel} \rangle = \frac{\int_{E}^{E^{max}} \zeta_{\parallel}(E_+, \xi_2) \frac{d\sigma(E_\gamma, E_+)}{dE_+} dE_+}{\int \frac{d\sigma(E_\gamma, E_+)}{dE_+} dE_+},$$

where the integrals are taken from the maximum of the energy of positrons $E_+^{max} = E_\gamma - 2\, m_0 c^2$ down to energy spectrum. This value is a function of polarization ξ_2 of initial gamma beam. The function $f\ (E_+)$ can be evaluated by

$$f = 1 - 2\ (1 - E_+ / E_+^{max})^2,$$

when $E_+/E_+^{max} \geq 0.5$.

In output file of CONVER also exists the value of positron energy when it was created, also the output value of the energy. Polarization of created particles calculated with the last formula for f, where used value of energy, when the particle was created. The losses of polarization for each particle at the output of the target of thickness $\delta = t/l_{X_0}$ was calculated by the formula

$$\xi_{\parallel 1}(s = \delta) = \xi_{\parallel 1}(s_1, E_{+0}) exp(-(\delta - s_1)/3X_0)$$

where $3X_0$ is the length of depolarization [7], i is the particle number and E_{+0} is initial energy of the particle.

Polarization of gammas is a function of angle between direction of motion and direction of observation. Since the direction of radiation is distributed within angle θ, measured from longitudinal axis of undulator $\theta \cong (1 + P_\perp^2)^{1/2}/\gamma$, there is some possibility for illumination of the target by the photons with low level of polarization.

For preparing of gamma flux of maximal possible polarization, it is necessary, as it was mentioned, to provide an angular separation of gammas. The degree of polarization for the first and second harmonics of radiation is a function of energy of the

photon (or angle of observation $\Theta = \gamma\theta$) [17]

$$\xi_{21} = \xi_{22} = \frac{2s-1}{1-2s+2s^2}$$

where $s = E_\gamma / E_\gamma^{max} = 1/(1 + \Theta^2/(1+p_\perp^2))$, $E_\gamma^{max} = 2\hbar\Omega\gamma^2/(1+p_\perp^2)$.

This function is represented in Table 1.

Table 1.

Polarization as a function of the energy of photon

s	0.0	0.1	0.2	0.3	0.4	0.5	0.6	0.7	0.8	0.9	1.0
ξ_2	-1.	-0.97	-0.88	-0.68	-.38	0.0	.38	0.68	0.88	0.97	1.

It is clear, that it has point anti symmetry around s = 0.5 .

For obtaining the mean degree of polarization of the gamma flux, illuminated the target, it is necessary to averaged the values for ξ_{2n} in such manner as following

$$\langle \xi_{2n} \rangle = \frac{\int_s^1 \xi_{2n}(s) \frac{dN_{\gamma n}}{ds} ds}{\int_s^1 \frac{dN_{\gamma n}}{ds} ds}, \qquad (1)$$

where the integral in denominator of the last expression is the number of the photons emitted in the range of relative frequency s. In case $p_\perp^2 \ll 1$ expressions for spectral distribution are [17]

$$\frac{dN_{\gamma 1}}{ds} = \frac{2\pi\alpha\ Kp_\perp^2}{(1+p_\perp^2)^2} (1 - 2s + 2s^2),$$

$$\frac{dN_{\gamma 2}}{ds} = \frac{8\pi\alpha\ Kp_\perp^2}{(1+p_\perp^2)^3} s(1-s)(1 - 2s + 2s^2)p_\perp^2 \qquad (2)$$

The number of the photons emitted by the particle in the undulator on the n-th harmonic in the range of the relative frequency (1÷s) is

$$\Delta N_{\gamma n}(p_\perp, s) = \int_s^1 \frac{dN_{\gamma n}}{ds} ds = 4\pi\alpha n K \frac{p_\perp^2}{1+p_\perp^2} \Phi_n(p_\perp, s), \qquad (3)$$

where in the approximation $x = 2p_\perp \sqrt{s(1-s)/(1+p_\perp^2)} \ll 1$,

$$\Phi_1(p_\perp,s) = \frac{1}{6}(1-s)(2-s+2s^2) - \frac{p_\perp^2}{2(1+p_\perp^2)}(1-s)^2\left(\frac{4}{15}+\frac{8s}{15}-\frac{s^2}{5}+\frac{2s^3}{5}\right)$$

$$\Phi_2(p_\perp,s) = \frac{p_\perp^2}{10(1+p_\perp^2)}(1-s)^2\left[(1+2s-2s^2+4s^3) - \right.$$

$$\left. - \frac{20\,p_\perp^2}{21(1+p_\perp^2)}(1-s)\left(\frac{2}{15}+\frac{2}{5}s+\frac{4}{5}s^2-s^3+2s^4\right)\right].$$

Substituting in (1) expressions (2) for the first harmonic, we obtain for the case $p_\perp^2 \ll 1$ the mean degree of polarization $\langle\xi_{21}\rangle_s$ of the photon beam with energy range (1÷s), or corresponding angles

$$\langle\xi_{21}\rangle_s = \frac{3s}{2-s+2s^2}$$

This function is represented in Table 2.

Table 2.

Avegage polarization of the photon flux for the first harmonic

s	0.0	0.1	0.2	0.3	0.4	0.5	0.6	0.7	0.8	0.9	1.0
$\langle\xi_{21}\rangle$	0.0	0.16	0.32	0.48	0.63	.75	.84	0.92	0.96	0.99	1.

For estimation the value of polarization of the second harmonic, it is necessary to take into account, that the maximum of energy of the first harmonic corresponds to s = 0.5 for the second one. Nevertheless, as we accept the photons in selected angle $\theta < \theta^* = (\sqrt{1+p_\perp^2}/3)$ which namely corresponds to $s = E_\gamma/E_\gamma^{max} = \frac{1}{1+1/9} = 0.9$, and it does not depend of the harmonics number. So the only particles, *burned in the target* by the photons of the second harmonic with the half relative energy can also pass the selection system with the polarization close to 0.5 as it can be concluded from value for the $f \cong 1 - 2(1-1/2)^2 = 1/2$. Namely this particles lowering the level of polarization in output flux.

The mean polarization of the photon flux on the second harmonics, calculated with (1)-(3) is equal

$$\langle\xi_{22}\rangle_s = \frac{5\,s^2}{1+2s-2s^2+4s^3}.$$

This function is represented in Table 3.

Table 3.

Avegage polarization of the photon flux for the second harmonic

s	0.0	0.1	0.2	0.3	0.4	0.5	0.6	0.7	0.8	0.9	1.0
$\langle\xi_{22}\rangle$	0.0	0.042	0.148	0.29	0.46	.62	0.77	0.89	0.95	0.988	1.

The total number of the photons, emitted on the first harmonic is defined by previous relation with parameter s = 0 (i.e. integration from point s = 1 to s = 0) [17]

$$N_{\gamma 1} = \Delta N_{\gamma 1}(s=0) = \frac{4\pi\alpha K}{3}\frac{p_\perp^2}{1+p_\perp^2}\left(1-\frac{2}{5}\frac{p_\perp^2}{1+p_\perp^2}\right)$$

On Table 4 there is represented the number of the photons on the first and second harmonics for different $p_\perp$ and s factors, calculated with (3) for number of periods $K = 10^4$. This Table also can be used for estimation the number of the photons *outside* the angle of separation, which is important for calculation of the energy absorption in the diaphragm. For example, if the angle of selection for radiation is $\theta^*/3 = (1+p_\perp^2)^{1/2}/3$, which corresponds to s = 0.9 , i.e. collection in the range about 10% around the maximal energy of the gamma-quanta, then for $p_\perp = 0.5$, approximately 8 photons comes to the target and (56-8) = 48 heat the diaphragm. The energy of this photons is distributed correspondly to s factor value.

Table 4.

Number of the photons on the first and the second harmonics. Number of periods $K=10^4$

	$p_\perp$ =	0.7	0.5	0.35	0.2	0.1
s=0.9	ΔN_1	13.	8.2	4.4	1.59	0.41
	ΔN_2	1.6	0.59	0.18	0.02	.0014
s=0.8	ΔN_1	23.4	14.6	8.1	2.89	0.75
	ΔN_2	5.2	1.98	0.58	0.073	0.005
s=0.7	ΔN_1	31.3	19.8	11.1	3.98	1.032
	ΔN_2	9.6	3.6	1.1	0.13	.009
s=0.6	ΔN_1	37.8	24.1	13.6	4.9	1.27
	ΔN_2	14.3	5.37	1.6	0.2	0.013
s=0.5	ΔN_1	43.	28.1	15.9	5.79	1.5
	ΔN_2	19.	7.15	2.15	0.27	0.018
s=0.	ΔN_1	87.	56.2	31.9	11.6	3.0
	ΔN_2	38.	14.6	4.3	0.54	0.036

We can see from this table that angle selection over $\theta < \theta^*/3$ (s < 0.9) deceases the number of the photons on the first harmonic but also improves ratio $\Delta N_1/\Delta N_2$. Notice here that with

decreasing the $p_\perp$ factor also decreases the angle $\Theta^* = \sqrt{1+p_\perp^2}$. For estimation of the radius of the diaphragm for this angle of separation $s \approx \Theta^*/3$ ($s \approx 0.9$) we can write

$$r^* \cong L\,\Theta^*/3/\gamma,$$

where L is the distance from the end of the undulator to the target, which is of the order of the length of the undulator. Substitute here $L \cong 200$ m, $\gamma \cong 3\ 10^5$ (150 GeV), we obtain $r^* \cong 0.023$ cm or 0.46 mm in diameter. As it was shown (Table 2) the mean degree of polarization in the sport of such diameter is about 99%. Lowering the s value to 0.8, which corresponds to the angle $\Theta = ((1+p_\perp^2)(1/s-1))^{1/2} = \Theta^*(1/s-1))^{1/2} \cong 0.\ \Theta^* \approx 0.52$, the value of the diameter increase to 0.7 mm. The mean value of polarization of the photon flux on the first harmonics will be 96% and 95% on the second one.

From the Table 4 yields, that utilization of $p_\perp = 0.7$ and the diaphragm which gives $s = 0.1$ ($\Theta = \Theta^*/3$), provides the same ratio $\Delta N_1/\Delta N_2$ as for $p_\perp = 0.35$ without angular selection ($s = 0$). But the number of positrons in case $p_\perp = 0.7$ is tree times bigger, than for $p_\perp = 0.35$.

This is strong argument for increasing the $p_\perp$ value and usage of the diaphragm for shortening the length of the undulator (down to 50÷70 m) and saving polarization of the order 70÷80% .

If the distance from the undulator to the target increased, then, for the same angle of separation, the sport size also increase. Considerable may be the distance of the order of *one or two (few) kilometers*. In that case the condition of angular separation for radiation from the both ends of the undulator became the same. We will consider this question in other place.

4. NUMERICAL CALCULATION

For numerical calculation there was used program CONVER [10], which operates with files, obtained with program UNIMOD2 [13]. UNIMOD2 code simulates the processes pair production, Compton effect, photo effect with accuracy better than 1% (more accurate

formulas, than those written in chapter 2 for qualitative discussion). There was made some modification, which made possible to output coordinates of the particle, when it leaves the target, direction, the energy when the particle was created, output energy, number of generation and distance, when particle created. File from CONVER is used by other code OBRA, in which calculation of all necessary parameters is organized, including polarization of the beam and heating of material of the target. For material of the target can be used any one. This choice of material must be made in code UNIMOD2 and the output file marks the material used. Practically in PC, there are formed few sub-directories, which contains the output files from UNIMOD2 for different materials and different energy of the photon beam.

The types of targets used in calculation are represented on Fig.2.

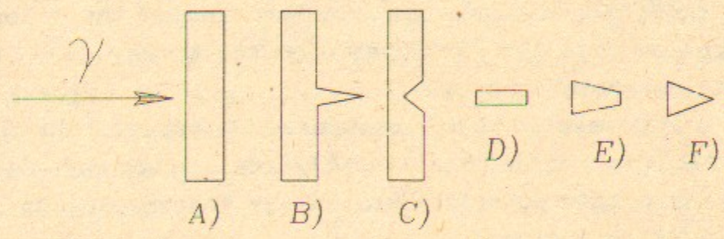

Fig.2. Types or targets used for calculation.

Types of B) and C) used for modeling erosion of the material. Types D), E) and F) were investigated following naive idea, that scattered positrons goes away from the target trough side walls. The design of the targets of these last types means, that they are mounted in the envelope material with low Z (Beryllium).

General output from this consideration is that the efficiency is approximately *the same* for all types of the targets.

In Tables 5-7 there are presented parameters of conversion of photons into particles when the gammas have initial energy 40 MeV.

Collected energy is equal to 30 ± 10 MeV. That is preliminary separation. Material of the target used here is Tungsten.

Briefly remind here the physical properties of this material, which we are using in OBRA.

W (Tungsten):

Atomic number	74
Atomic mass	183.85 (5 isotopes: 180,182,183,184,186)
Radiation Length X_0	6.8 g/cm^2, $l_{X_0} \cong 0.35$ cm.
Heat capacity c_p	20.53÷26.9 Joules/moll/deg(t≈150÷1500 ^{0}C)

——— Additional figures ———

Density	19.3 g/cm^3
Melting temperature	3370 ^{0}C
Heat conductivity	130÷92 W/m/deg (t≈ 27÷2427^{0}C)
Young's modulus	35000÷38000 kg/mm^2
Tensile strength	100 ÷430 kg/mm^2

Angle of preliminary collection ϕ for Table 5: ϕ = ± 0.1 rad, for Table 6: ϕ = ±0.5 rad, for Table 7 ϕ = 1.0 rad. Total number of generated photons is 5561 for this energy. In the data files there are included only particles, which have energy in the acceptance interval. That was made for shortening the files, cause *final* separation cuts the particles with the energy less, than one half of initial photon energy.

Here are presented the thickness of target (in units of radiation length), efficiency, statistical error of calculated efficiency, effective polarization, mean energy losses in units Mev/particle. σ_γ = 0.05 cm.

Table 5.

E_γ=40 MeV, E_+ = 30 ±10 MeV, ϕ = ± 0.1 rad

t,cm	t/l_{X_0}	$k/10^{-2}$	$\delta/10^{-3}$	$<\zeta>$	ΔW, MeV/e$^+$
0.05	0.14	2.50	2.13	0.83	0.327
0.10	0.28	3.2	2.40	0.832	0.504
0.15	0.43	4.14	2.73	0.803	1.22
0.20	0.57	2.93	2.30	0.805	0.96
0.25	0.71	2.23	2.48	0.805	0.743
0.30	0.85	2.18	2.40	0.799	0.705
0.35	1.00	2.00	2.32	0.814	1.14
0.40	1.14	2.02	2.29	0.796	1.44

Table 6.

E_γ=40 MeV, E_+ = 30 ±10 MeV, ϕ = ± 0.5 rad

t,cm	t/l_{X_0}	$k/10^{-2}$	$\delta/10^{-3}$	$<\zeta>$	ΔW, MeV/e$^+$
0.05	0.14	2.72	2.20	0.816	0.47
0.10	0.28	4.50	2.86	0.802	1.21
0.15	0.43	6.10	3.30	0.789	2.21
0.20	0.57	6.47	3.50	0.781	2.32
0.25	0.71	6.04	3.40	0.774	2.92
0.30	0.85	5.89	3.40	0.772	2.86
0.35	1.00	5.01	3.20	0.778	3.22
0.40	1.14	4.65	3.00	0.772	3.28

Table 7.

E_γ=40 MeV, E_+ = 30 ±10 MeV, ϕ = ± 1.0 rad

t,cm	t/l_{X_0}	$k/10^{-2}$	$\delta/10^{-3}$	$<\zeta>$	ΔW, MeV/e$^+$
0.05	0.14	2.71	2.21	0.814	0.47
0.10	0.28	4.59	2.87	0.8	1.25
0.15	0.43	6.20	3.34	0.785	2.31
0.20	0.57	6.96	3.54	0.778	2.57
0.25	0.71	6.71	3.40	0.772	3.21
0.30	0.85	6.62	3.45	0.766	3.22
0.35	1.00	5.88	3.24	0.771	3.67
0.40	1.14	5.38	3.00	0.765	3.73

On Table 8 there is represented calculated dependence of conversion efficiency on thickness of the target, which gives maximum yield of positrons as a function of the angle of capture. Here also represented the temperature gain per captured positron of the pair. That figure is averaged over *all* volume, where energy deposits (like all particles created at the entrance of the target). If we take into account approximately linear gain of the number of created positrons inside the target, for maximal gain of the temperature at the output of the target it is necessary to multiply this figure by the factor of tree.

For real estimation of temperature it is necessary also to take into account the low energy part of the spectrum of created particles. Calculation of such type was also made with program UNIMOD2, where was taken into account all this factors, see lower (page 28).

Table 8.

E_γ = 40 MeV, t/X_0 = 0.57

ϕ,rad	$k/10^{-2}$	$\delta/10^{-3}$	$<\zeta>$	Δ W, MeV/e^+	Δ T,deg /10^{-1}/2e
1.00	6.96	3.56	0.778	2.57	14.5
0.80	6.94	3.55	0.779	2.56	14.6
0.60	6.71	3.52	0.779	2.40	13.9
0.50	6.45	3.50	0.781	2.38	14.1
0.40	6.05	3.44	0.784	2.23	14.5
0.30	5.21	3.30	0.788	1.93	13.8
0.20	4.23	3.06	0.792	1.68	13.6
0.10	2.96	2.70	0.805	0.96	11.2

On Fig.3. there is made graphical representation of the efficiency for all these angles of capture for energy of the quanta of 40 MeV.

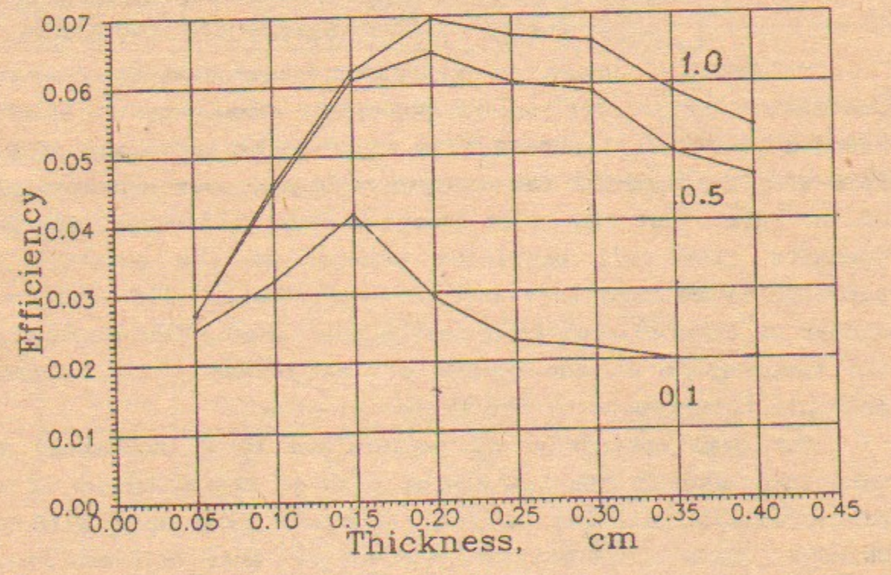

Fig.3. Efficiency as a function of the thickness for different captured angle.

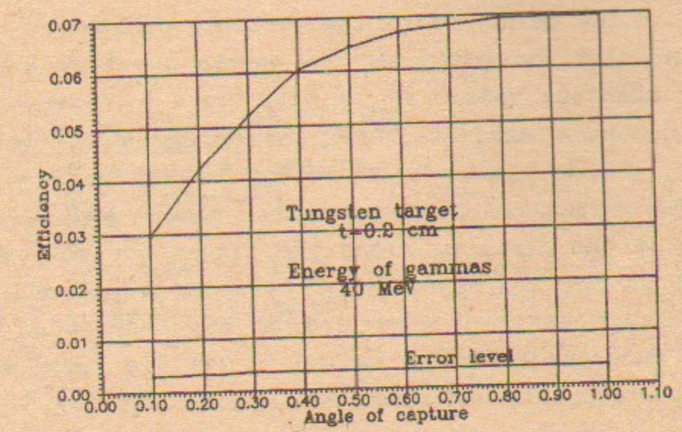

Fig.4. Efficiency as a function of the captured angle. Energy of the quanta E_γ = 40 MeV.

From Table 8 and Fig.4, where the data are represented in graphical form, one can see, that practically, angle of capture about $\phi = \pm(0.3 \div 0.4)$ rad is enough for successful operation.

Effective thickness can be estimated though effective angle spread, produced by the target according to angular distribution at output of the target of thickness δ (for plane angle θ)

$$F(\theta)\, d\Omega \cong \frac{1}{\sqrt{\pi}\,\theta_0} \exp(-\theta^2/\theta_0^2)\, d\theta$$

where θ_0

$$\theta_0^2 \cong (20/p\beta)^2 \delta \cdot (1 + \tfrac{1}{9} \log_{10}\delta)^2 \text{ [radians]}^2,$$

and p are taken in MeV/c. If we estimate from Fig.4, which may be considered as integral of the F function over θ, the effective angle of divergence as $\theta_0 \cong 0.2$ rad, then for pc = 20 MeV we can calculate from last equation δ = 0.05 (or 0.05·0.35 = 0.0175 cm).

Direct numerical calculations with OBRA follows the simple algorithm as

$$L_{eff} = \frac{\sum_{i=1}^{N} (t - s_i)}{N},$$

where N - is a full number of particles in consideration, t - is

the thickness of the target, s_1 is the distance from the beginning of the target to the point, where the particle created $0 < s_1 < t$.

At the intermediate energy of the quanta about 20 MeV $L_{eff} \cong$ $\cong 0.35\ t$, and absolute value $L_{eff} \cong 0.35 \cdot 0.2 \cong 0.07$ cm, i.e. the effective thickness, estimated over angular spread is *less*.

On Fig.5, Fig.6 there is represented the distribution of quantity of the particles, produced in the target and leaving it, as a function of the distance along the target for energy of the gammas 40 and 20 MeV correspondly. This Figures are illustrated the previous consideration at the end of the Chapter 2, showing the nonlinear dependence of the number of created particles (and which leave the target in the range of angle acceptance) along the distance in the target.

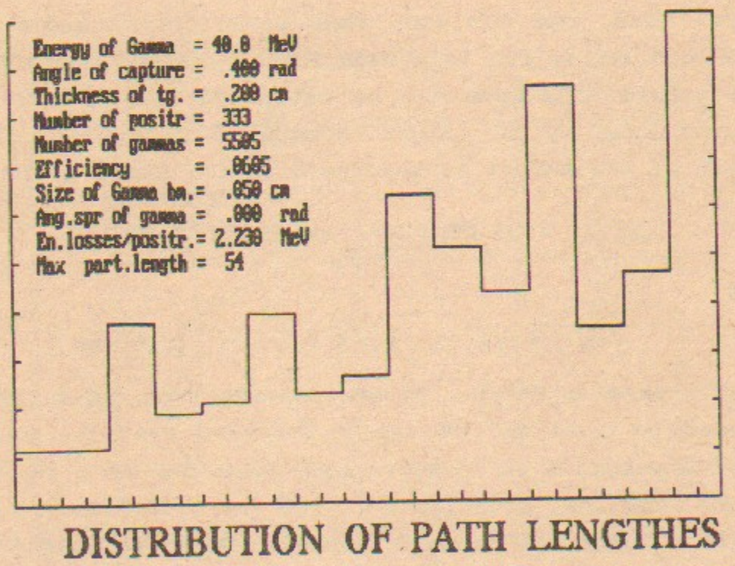

Fig.5. Number of created particles as a function of the distance along the target for gammas of 40 MeV. Left and right axis corresponds to the surface of the target (left-entrance).

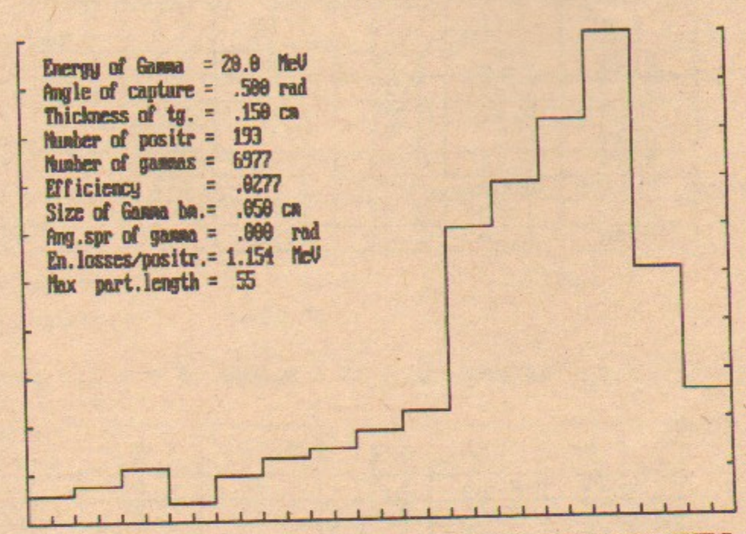

Fig.6. Number of created particles as a function of the distance along the target for gammas of 20 MeV.

On Tables 9-11 there are represented the same parameters, as in Tables 4-6, but for the energy of quanta E_γ = 20 MeV. Number of gammas, used here was N_γ = 6992, σ_γ = 0.05 cm.

Table 9.

E_γ = 20 MeV, E_+ = 15 ± 5 MeV, ϕ = ± 0.1 rad

t,cm	t/l_{X_0}	$k/10^{-2}$	$\delta/10^{-3}$	$< \zeta >$	Δ W, MeV/e^+
0.01	0.028	0.42	0.78		
0.025	0.07	0.95	1.23	0.809	0.16
0.05	0.14	1.14	1.43	0.799	0.22
0.10	0.28	1.13	1.41	0.807	0.33
0.15	0.43	1.25	1.56	0.8	0.19
0.20	0.57	1.20	1.51	0.801	0.34
0.25	0.71	1.02	1.40	0.791	0.23
0.30	0.85	1.00	1.42	0.824	0.38
0.35	1.00	1.03	1.49	0.788	0.21
0.40	1.14	0.89	1.36	0.791	0.42

Table 10.

E_γ= 20 MeV, E_+ = 15 ± 5 MeV, ϕ = ± 0.5 rad

t,cm	t/l_{Xo}	$k/10^{-2}$	$\delta/10^{-3}$	$<\zeta>$	$\Delta W, MeV/e^+$
0.05	0.14	1.83	1.64	0.817	0.61
0.10	0.28	2.36	1.94	0.814	1.05
0.15	0.43	2.77	2.11	0.81	1.15
0.20	0.57	2.56	2.12	0.805	1.35
0.25	0.71	2.43	2.04	0.808	1.41
0.30	0.85	2.39	1.99	0.81	1.28
0.35	1.00	2.50	2.05	0.799	1.23
0.40	1.14	2.05	1.92	0.802	1.45

Table 11.

E_γ= 20 MeV, E_+ = 15 ± 5 MeV, ϕ = ± 1.0 rad

t,cm	t/l_{Xo}	$k/10^{-2}$	$\delta/10^{-3}$	$<\zeta>$	$\Delta W, MeV/e^+$
0.05	0.14	1.87	1.64	0.816	0.64
0.10	0.28	2.72	1.97	0.807	1.20
0.15	0.43	3.36	2.19	0.809	1.44
0.20	0.57	3.24	2.16	0.803	1.62
0.25	0.71	3.15	2.12	0.8	1.73
0.30	0.85	2.91	2.04	0.808	1.67
0.35	1.00	2.92	2.05	0.796	1.45
0.40	1.14	2.67	1.96	0.8	1.76

With this tables we can estimate, for example, the input from the second harmonic for energy of gammas of the first one equal to 20 Mev. Let the s factor will be s = 0.9, and $p_\perp$ = 0.7, angle of capture $\phi \cong \pm 0.5$ rad and the thickness t/l_{Xo} = 0.5 - optimal for this energy. From the Table 4 we found, that the number of the quanta, created by one initial electron or positron on the first harmonic will be $\Delta N_1 \cong 13$ and on the second $\Delta N_2 \cong 1.6$ with $\xi_{21,22} \cong 0.99$. This 13 quanta of 20 MeV will give $\cong 13 \cdot 0.03 = 3.9$ positrons with polarization ≅ 80% . The quanta from the second harmonic with energy 40 MeV will give $\cong 1.6 \cdot 0.06 = 0.096$ positrons with polarization about 50%, as we collect the only particles near maximum of the first harmonic. So, the resulting polarization will be

$$P=\frac{[3.9\cdot(0.8+0.1)+0.096(0.5+0.25)] - [(3.9\cdot 0.1+0.096\cdot 0.25)]}{[3.9\cdot(0.8+0.1)+0.096(0.5+0.25)] + [(3.9\cdot 0.1+0.096\cdot 0.25)]} = 0.79,$$

i.e. 79%.

In the Table 12 there is represented the results of calculation of the efficiency for Titanium target. This calculations initiated by the proposal [15] to use material of target with small Z, but the same ratio t/X_0 , cause formally the efficiency depends of the thickness of the target with this combination. The reason for usage of light materials -the bigger heat capacity due to Dulong-Petite law.

The properties of Titanium are represented by following

Atomic number 22
Atomic mass 47.9
Radiation Length X_0 16.1 g/cm^2; $l_{Xo} \cong$ 3.55 cm.
Melting temperature 1660 ^{0}C
Density 4.54 g/cm^3
Heat capacity c_p 25.02 Joules/moll/deg(t≈150÷1500 ^{0}C)

Table 12.

E_γ= 20 MeV, E_+ = 15 ± 5 MeV, ϕ = ± 0.5 rad
Material of the target -Ti N_γ = 9997

t,cm	t/l_{Xo}	$k/10^{-2}$	$\delta/10^{-3}$	$<\zeta>$	$\Delta W, MeV/e^+$
0.25	0.07	0.79	0.89	0.813	0.33
0.5	0.14	1.31	1.15	0.829	1.17
1.0	0.28	1.73	1.31	0.817	1.63
1.5	0.42	1.54	1.24	0.84	1.64
2.0	0.56	1.50	1.23	0.829	1.86
2.5	0.70	1.48	1.22	0.826	1.72
3.0	0.84	1.45	1.21	0.81	1.52
3.55	1.00	1.40	1.18	0.83	1.86

As it can be seen from this Table and, correspondly, Table 10, the efficiency for Ti target is lower for the same ratio t/X_0. This factor of decrease for t/X_0 = 0.28 is only about 30%. For this material efficiency is saturated at the thickness about 1 cm. This is due to domination of the scattering at the angles, bigger, than the angle of capture. So as the energy deposition per particle is approximately the same, the temperature gain will be lower at 10·183/47·0.7 = 27 times. The factor 10 reflects increase the real size of the target, 183/47 shows the ratio of heat capacities, and 0.7 reflects the decrease of efficiency. This figures looks optimistic.

On the Fig.7-9 there is represented the energy distribution of created particles (i.e. at the very moment of creation) and output distribution for quanta of 40, 20 and 10 MeV for Tungsten.

Distribution of the particle with defined level of polarization is represented on Fig.10 for quantum energy 40 MeV. Solid line shows graph of polarization, the same as Fig.1, dotted line shows energy distribution, the same as Fig.7, and last curve shows distribution of polarization of output beam, versus fractional energy, counted from maximum of the energy spectrum.

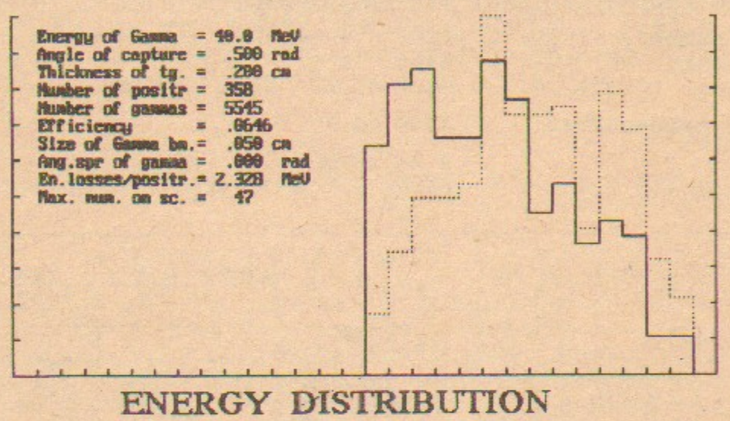

Fig 7. Positron energy distribution for quanta of 40 MeV. Dotted curve shows distribution at the creation point

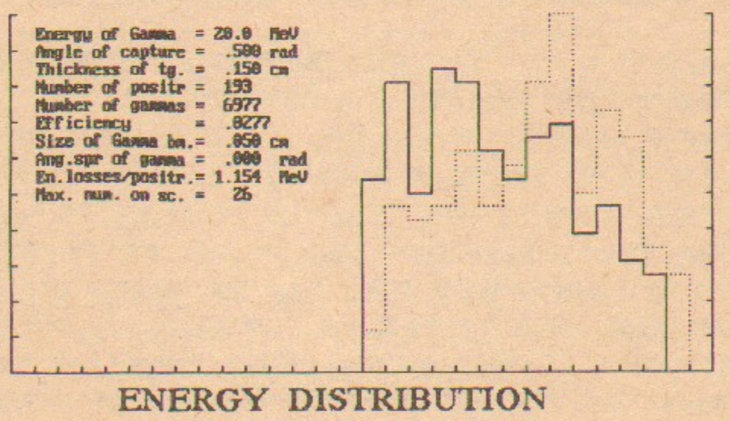

Fig.8. The same as at Fig.7, for energy of the quanta 20 MeV.

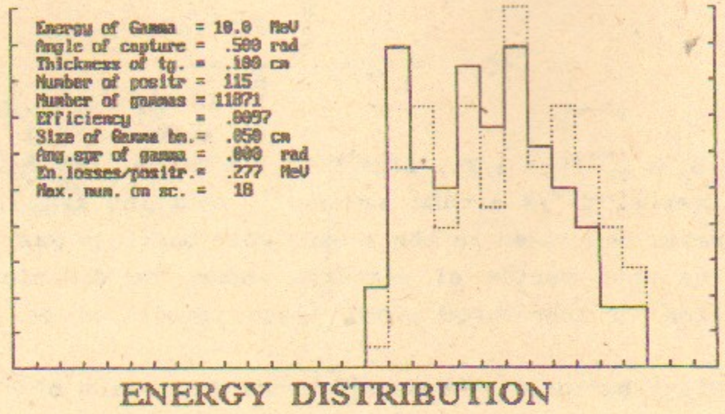

Fig.9. The same as at Fig.7, for energy of the quanta 10 MeV.

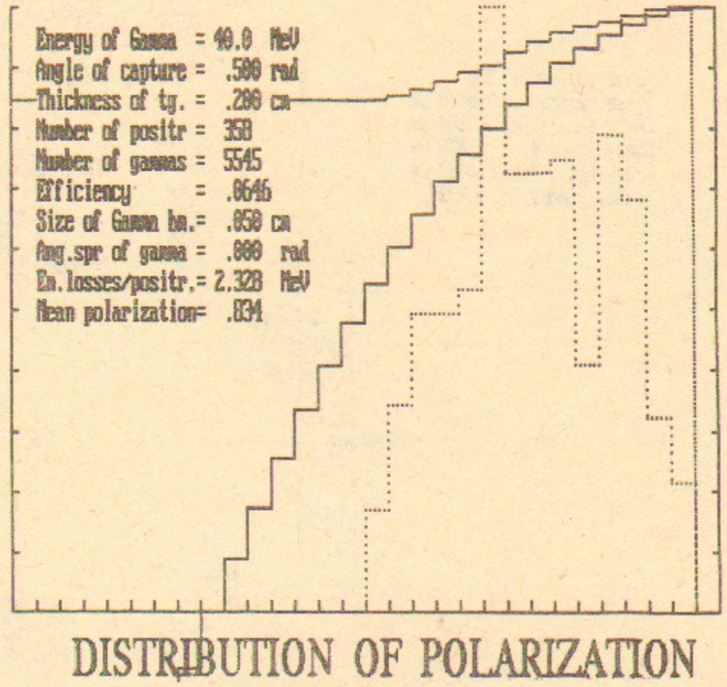

Fig.10. Distribution of polarization. There is shown the curve for *f* -function, end distribution over energy, at the moment of creation of the particles.

Namely on Fig.10 there is represented the function

$$\langle \zeta_{\parallel} \rangle = \langle \xi_2 \rangle \frac{\sum_{1}^{N} f(E_+^i)\Delta N(E_+^i)}{\sum_{1}^{N} \Delta N(E_+^i)}$$

here $E_+^i = E_+^{max}(1 - i/N)$, $\Delta N(E_+^i)$ is the number of the particles in ne interval E_+^{max}/N around energy E_+^i, counting from the E_+^{max}. Here ne energy was taken in the moment *when particle was created.*

The next series of pictures shows the distribution of the articles in transverse phase space, projected on corresponding xis.

Distribution of the particles as a function of the transverse omenta is represented of Fig.14. Here used target of Tungsten of $4X_0$ thickness for gammas of 40 MeV. With dot line there is shown stribution for one direction, P_x, with solid line - value of ull transverse momenta $P_\perp^2 = P_{\perp x}^2 + P_{\perp y}^2$.

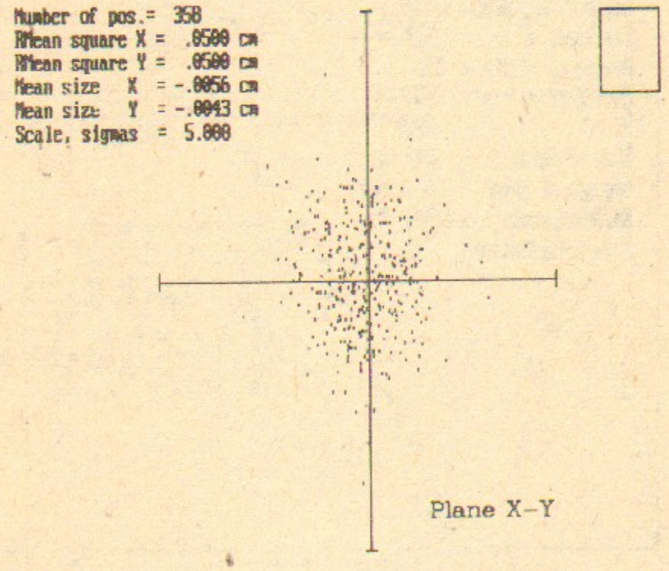

Fig.11. X-Y distribution, i.e. transverse distribution in real space. Figure in the right upper corner is square, and pictured for calibration of scales in two directions.

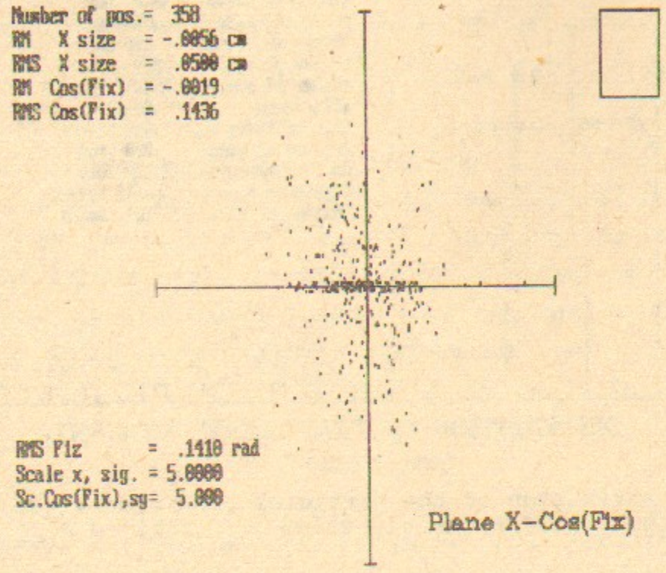

Fig.12. X-Cos X' distribution

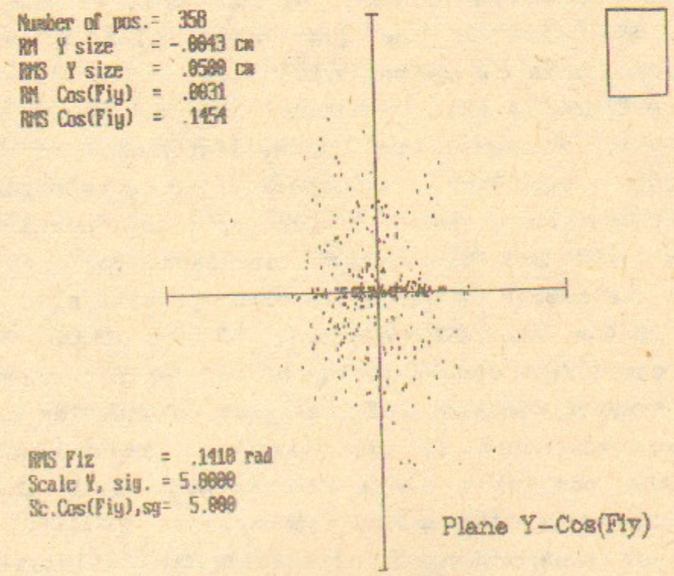

Fig.13. Y-Cos Y' distribution

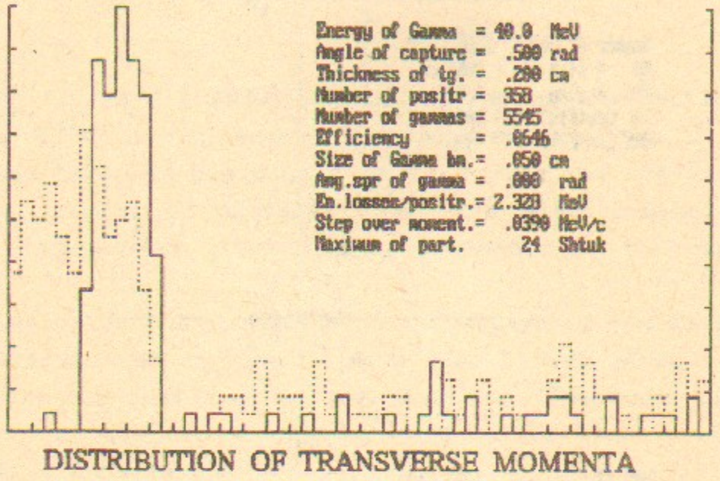

Fig.14 Distribution of the particles over transverse momenta, Dotted line-for one direction $P_{\perp x}$. Solid - $P_{\perp}^2 = P_{\perp x}^2 + P_{\perp y}^2$.

For calculation of the heating, with the code OBRA there is used averaged dimensions of the positron sport at the output of the target. The size of the gamma-ray, which illuminate the target, is less, than the output sport size, so for calculation of the volume there is used formulas for cut cone. The energy deposition, which is represented in the last column of the Tables, divided by this volume and heat capacity. It is necessary to take into account, that total number of the particles, heats the target is bigger at least four times, that calculated for each positron. First of all the number of particles with opposite sign of charge (electrons) is the same. This gives the factor of two. The other factor of 2 comes from consideration of soft energy spectra, which is cut in CONVER for decrease of the files volume. The main factor defined the temperature is approximately linear increase the number of the particles along the target which gives qubic function of the temperature along the target.

For direct calculation of the heating for calibration of the factors we used the general code UNIMOD2, which also has this possibility. The results are the following.

For collimated gamma-ray with uniform distribution of 0.05 cm in diameter at the entrance of the target, the average energy deposition at *the end of the target* is about 250 MeV/gramm. The thickness of the target was chosen of 0.2 cm, the energy of gammas used is equal to 20 MeV. This deposition corresponds to heating

$$\Delta T = 250\ 1.6\ 10^{-19}\ 10^{6}\ 183\ /25. = 2.928\ 10^{-10}\ \text{deg/photon}.$$

For obtaining resulting efficiency for positron production, equal to unity, it is necessary to use ≅ 1/0.0256 = 39.0 photons per one positron at the output, so the temperature gain will be $\Delta T = 2.928\ 10^{-10} \cdot 39. = 1.14\ 10^{-8}$ deg/e^+. This yields that output plane of the target has a heating up to 116 deg for the beam of 10^{10} positrons (or electrons) in operation per one initial bunch. For Titanium target this figures drops to 4.5 degrees.

5. COLLECTION

All previous Tables and pictures are obtained for the particles, which has energy spread from the half of the maximal energy to its maximal value. Further separation decreases the conversion efficiency, but increase the mean polarization.

First there was investigated the Lithium lens in [2]. The main output of this considerations is that the system of the Lens with quarter wave transformation and diaphragm can select the particles and give polarization at least 65% . This numerical calculations made for different thickness of the target and taken into account short focusing lens and acceleration in longitudinal field.

The possible schemes for collection of the particles are represented on the Fig 15 A) and B). So as absorption of the gamma-ray in the target is small it is possible to use *few targets* installed serially.

On Fig.15 A) there is shown variant with two targets for obtaining positrons and electrons from the same gamma- ray. This ray are going after the first target through the accelerating structure A, which has the holes in iris diaphragms, and the hole in back leg of the yoke of the bending magnet M. This magnet bends

away the straight line the created particles and directed its to separate beam lines. Short focus lens L collects the electrons or positrons from the target. The energy, gained by A is of the order of hundred MeV, i.e. bigger, than the energy spread of created particles.

On Fig 15 B) there is shown the scheme for summarizing the particles, obtained from two targets into one beam line. Here accelerating structures A_1 and A_2 provides different values of the beam energy E_1 and E_2 so, that E_1 is bigger, than E_2. Bending magnets M_1 and M_2 directed the beams to the magnet M_3. The relation between E_1 and E_2 and the angle of injection of each beam into M_3 are chosen is such manner, that provides the same output trajectories for these two beams with different energy. The difference of the lengths of the beams trajectories is equal to half wavelength of the acceleration structure A_3. The phase tuning is that the beam from the first target, which has bigger energy, is decelerating in A_3 and the second beam are accelerating. For this space separation of the beams the length of accelerating structure

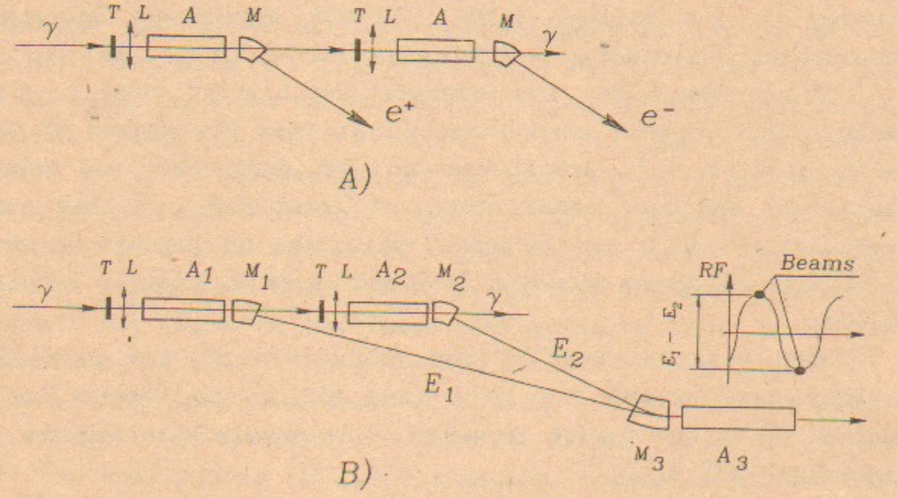

Fig.15. Possible schemes for conversion units.
T- target, L - short focusing lens, M_{1-3}- bending magnet, A_{1-3} -accelerating structure

is minimal for fixed gradient. After that these two bunches are injected in damping ring, for which such lengthening of the beam is useful at initial stage of cooling. Of course, the other path length of the trajectories for the beam number one and number two also possible, but requires the more length for accelerating structure A_2 (for fixed gradient in it).

On the Fig.16 there is represented principal view of the target device with *diaphragm*. Here we consider only main characteristics of it. First of all notice here that the diaphragm made by beryllium rod with round hole.

The properties of Beryllium represented by following

Atomic number	4
Atomic mass	9.01
Radiation Length X_0	63.9 g/cm^2, $l_{X_0} \cong$ 34.6 cm.
Melting temperature	1660 ^{0}C
Density	4.54 g/cm^3
Heat capacity c_p	16.4 Joules/moll/deg

The mean power of the gamma ray can achieve a few percents of the full power of the beam passing the undulator, so it can be of the order of a *hundred* kiloWatts. After cooled Beryllium rod there are two collimators with magnetized iron, for deflection of the electrons and positrons, created in the rod.

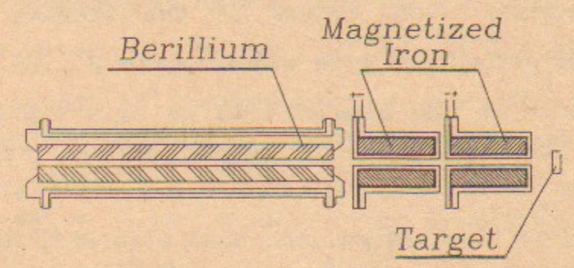

Fig.16. Principal view of the conversion unit with diaphragm.

The output file contains all necessary characteristics of particles to calculate its motion in following focusing system. More detailed description of this system will be done in other

place.

After preliminary acceleration in RF structure the collected particles go to damping ring for preparing low emittance beam. The prototype for such damping ring is described in [9].

6. PROPOSAL FOR SLAC ACCELERATOR

The method of polarized particle production can be tested at the energy, which is available at SLAC, which has maximal energy about 50 GeV, number of particles $N \cong 5\ 10^{10}$, emittance $\gamma\varepsilon \cong 3\ 10^{-3}$ rad cm. Such value of emittance makes possible to provide the beam of very small dimensions and, hence to use Undulator with small diameter of aperture. This makes possible to provide short period of the field in the undulator. Such as the energy of the quanta depends of the period λ_0

$$E_{\gamma_n}^{max} = n\ 2\ \gamma^2 \hbar\Omega/(1+P_\perp^2) \cong 2.48\ n\ (\gamma/10^5)^2/\lambda_0[cm]/(1+P_\perp^2)[MeV]$$

where $\Omega = 2\pi c/\lambda_0$ - is the angular frequency of transverse oscillations in the wiggler, n =1,2,..., there is possible to obtain the energy enough for operation, if λ_0 of the order of 0.1 cm can be fabricated.

If we suppose, that center of the wiggler installed in crossover of beta-function with significance β^*, so $\beta(l) = \beta^* + \frac{l^2}{\beta^*}$ and the beam size in the wiggler will be $a = (\gamma\varepsilon\ \beta/\gamma)^{1/2}$. If we assume, that the beam size at output of the wiggler is ≅10% bigger, than in crossover, i.e. $l^2/\beta^{*2} \cong 0.2$, that gives for l = 2 meters $\beta^* \cong l/(0.2)^{1/2} \cong 450$ cm. The beam size will be at energy 50 GeV, $a \cong (3\ 10^{-3}\ 450\ /10^5)^{1/2} = 3.7\ 10^{-3}$cm. The aperture of the vacuum chamber A let be ten times more i.e. $A = 3.7\ 10^{-2}$cm or 0.37 mm. So diameter of inner chamber of the wiggler will be at least 1 mm. This makes possible to have *period* λ_0 of 2 mm , $P_\perp \cong 0.2$ and correspondly, $E_\gamma \cong 2.48\ 5 = 12.4$ MeV.

Number of the quanta, radiated by N particles in the Undulator, described by the formula [17]

$$N_{\gamma_1} = N\ \frac{4\pi\alpha K}{3}\ \frac{p_\perp^2}{1+p_\perp^2}\ \left(1 - \frac{2}{5}\ \frac{p_\perp^2}{1+p_\perp^2}\right)$$

In our case $P_\perp^2/(1+p_\perp^2) = 0.038$, K= 400/0.2 and $N_{\gamma_1}/N \cong 2.3$ or 2.3 quanta per one initial particle for the undulator of 4 meters total length. The spectrum of radiation is good forming, cause $P_\perp$ is so small, and represented by the fist harmonic mainly.

In Table 13 there is represented the efficiency of conversion for gammas with E_γ = 10 MeV. Number of gammas used here is ≅11000.

Table 13.

E_γ= 10 MeV, E_+ = 7.5 ±2.5 MeV, ϕ = ± 0.5 rad

Target-tungnsten disk

t,cm	$\delta=t/l_{X_0}$	$k/10^{-2}$	$\varepsilon/10^{-3}$	$<\zeta>$	ΔW_+ MeV/e^+
0.01	0.028	0.34	0.54	0.78	0.007
0.025	0.07	0.74	0.78	0.79	0.05
0.05	0.14	0.95	0.87	0.79	0.26
0.10	0.28	1.14	0.98	0.79	0.51
0.15	0.43	1.04	0.98	0.79	0.48
0.20	0.57	0.93	0.87	0.786	0.56
0.25	0.71	0.77	0.80	0.798	0.61

0.299

The energy losses shown here cover the losses over *full* angle range, bun not only ± 0.5 rad.

So it is possible to obtain here for δ = 0.15

$$N_+/N = (N_+/N_\gamma)(N_\gamma/N) \cong 0.011\ 2.3 = 0.025,$$

which gives ≅1.25 10^9 positrons per one initial bunch.

The analytical expression of efficiency is [17]

$$\Delta N_{+1} \cong 3\ 10^{-2}\ k^2\ K\delta\ \frac{p_\perp^2}{1+p_\perp^2}\ \frac{y_f}{y_1}\ (1 - \xi_1),$$

where y_f and y_1 ($y_1 > y_f$) are the distance from the target to the end and to the entrance of the undulator correspondly, ξ_1 is the energy range of collected particles, calculated from maximal possible energy for positron (ξ_1 = 0 corresponds to full accepting of the particles), k is the factor which shows the part of θ^* usage (1/3 for s = 0.9). This formula are valid for thickness of the order $\delta \cong 0.1$ (for $E_\gamma \cong$ 10 MeV), where multyscattering is not sufficient and it also did not take into account *absorption* of the

positrons in the target. If we increase the distance from the target to undulator, so the $y_f/y_i \cong 1$ and estimate parameters $k \cong 1/3$, $K = 2\ 10^3$, $\delta = 0.15$, $p_\perp = 0.2$, $P_\perp^2/(1+p_\perp^2) = 0.038$, $\xi_1 = 0.9$, the conversion efficiency will be

$$\Delta N_{+1} \cong 3\ 10^{-2}\ 0.1\ 2\ 10^3\ 0.15\ 0.038\ \ 0.1 = 0.034,$$

slightly bigger, than estimated from numerical calculations. Here we must follow the results of numerical calculations.

The polarization of the *output beam* $\langle\xi_{21}\rangle$ will be of order $\langle\xi_{21}\rangle \cong 0.99\ 0.79 = 0.78$, as multiplication of polarization of the gamma ray and output polarization of the positrons as function of its initial energy.

So this value can be significant for *B-factory* of SLAC.

7.CONCLUSION

Of cause as we consider some general aspects of the calculation of the efficiency, not connected with any Project, the results also has general significance.

First of all there are developed new codes, which permits to calculate efficiency of conversion into polarized particles for different profile and material of the target.

Utilization of the diaphragm before target makes possible operation with the $p_\perp$ factor of the order 0.5÷0.7 .

Considerable may be the distance between the end of the undulator and the target of the order of one kilometer. This gives possibility to increase the sport size on the target.

For optimization of the heating it is desirable to work with slightly less thickness (of the order 10%) of the target than provides maximal efficiency of conversion. More radical will be usage of few targets and summarizing the particles in longitudinal phase space.

Optimized thickness of the target depends of the energy of the gamma-quanta, provided by undulator and lies in region 0.25÷0.57 l_{X_0} for gammas of 10÷40 MeV.

The mean degree of polarization can achieve 75÷80%.

For not polarized particles needs after conversion the length can be shorter as a result of absence the necessity of energy selection and, mainly, the possibility to make the $P_\perp$ factor bigger, remember that total number of the photons emitted is proportional to $P_\perp^2$ for low $p_\perp$. For $p_\perp \geq 1$, number of the photons, radiated on the n-th harmonic is proportional to $n^{-2/3}$.

Utilization of Titanum as a material for target promisses drastical decrease of the temperature gain for one pulse, decreasing the efficiency only on 30÷40%.

The method of polarized particle generation is open for application in any Linear Collider. As the technology of fabrication of the wiggler with superconducting coils and short period about 0.5 cm is not a problem now [5], it is possible to obtain polarized particles without serious restrictions. Thermal effects are also reduced for particles production with this method.

This makes possible utilization of this method of particles production, first proposed for VLEPP, in CLIC, DESY/THD, KEK, TLC, TESLA.

Proposal for SLAC linac shows that the amount of created positrons is of the order of 2÷3% of initial beam *for single target*. Resulting polarization is about 70%. This amount can be considerable for production of polarized particles *in B-factory* of SLAC.

8. REFERENCES

1. Conversion system for obtaining highly polarized electrons and positrons, Preprint INP 79-85, Novosibirsk 1979.
   V.E.Balakin, A.A.Mikhailichenko: VLEPP. The Conversion System, Proc. of the 12 Int.Conference on High Energy Accelerators, Batavia,1983,p.127.
2. *A.D.Cherniakin et al.*:Development of the conversion system for VLEPP project, ibid., p.131.
3. *T.A.Vsevolojskaya, A.A.Mikhailichenko, E.A.Perevedentsev, G.I.Silvestrov, A.D.Cherniakin*: Helical Undulator For Conversion system of the VLEPP project, Proc.of the 13 Int. Conference on High Energy Accelerators, Novosibirsk, 1989, vol.1, p.164
4. *A.A.Mikhailichenko*: Polarized e^+,e^- production, Proceedings

of Capri Workshop on Linear Colliders, Capri, 1988.
5. *A.A.Mikhailichenko*: Conversion System for Obtaining Polarized e^+,e^- at High Energy, Dissertation, Novosibirsk, INP, 1986.
6. *D.E.Alferov, Yu.A.Bashmakov, K.A. Belovintsev, E.G.Bessonov, P.A.Cherenkov*: The undulator as a source of electromagnetic radiation,Particle accelerators, 1979, vol.9, p.223.
7. *V.N.Baier,V.N.Katkov,V.S.Fadin*: Radiation of the relativistic electrons, Moscow, Atomizdat, 1973.
9. *V.V.Anashin,et al.*:Prototypes for the Damping Rings and the Beam Buncher Incorporated in the VLEPP Project, Proc. of the 13 Int. Conf.on High Energy Acc.,Novosibirsk,1989,vol.1,p.159.
10. *Bukin A.D.*:Choice of optimal Positron Converter for low Energy Beam (in Russian), Preprint INP 90-100.,Novcsibirsk, 1990.
11. *B.F.Bayanov, G.I.Budker et al*: Powerful optics with large magnetic fields for effective production of the beams of secondary particles, Preprint INP 79-149, Novosibirsk, 1979.
12. *A.I.Akhiezer, V.B.Berestetzki*: Quantum Electrodynamics, Moscow, Nauka, 1981.
13. *A.D.Bukin, N.A.Grozina, M.S.Dubrovin e.a.*: UNIMOD2 - Universal Simulating Program for e^+e^- experiments (in Russian), Manual, Novosibirsk, 1990, Preprint INP 90-93.
14. *A.A.Mikhailichenko, V.V.Parkhomchuk*: Transverse Resistive Instability of a Single Bunch in Linear Collider, Preprint INP 91-55, Novosibirsk, 1991.
15. *K.Flöttmann, J.Roßbach*: A high Intensity Positron Source for Linear Collider, DESY M-91-11, 1991.
16. *G.I. Sil'vestrov*: The problems of obtaining the Intense secondary beams, XII International Conference on High energy Accelerators, Novosibirsk, 1986.
17. *E.G Bessonov, A.A.Mikhailichenko*: Some aspects of Undulator radiation forming for conversion system of the Linear Collider BudkerINP 92-43, Novosibirsk, 1992.
18. *V.A.Tajursky*: EMSH-code for calculation of passing the electrons and photons at 10 keV-1Tev energy range, Preprint INP 98-16, Novosibirsk, 1989.

OPTIMIZED TARGET STRATEGY FOR POLARIZED ELECTRONS AND POSITRONS PRODUCTION FOR LINEAR COLLIDER

A.D.BUKIN, A.A.MIKHAILICHENKO

ОПТИМАЛЬНЫЙ ВЫБОР МИШЕНИ ДЛЯ ПОЛУЧЕНИЯ ПОЛЯРИЗОВАННЫХ ЭЛЕКТРОНОВ И ПОЗИТРОНОВ ДЛЯ ЛИНЕЙНОГО КОЛЛАЙДЕРА

А. Д. БУКИН, А. А. МИХАЙЛИЧЕНКО

ИЯФ 92-76

Работа поступила 19.X- 1992г.

Ответственный за выпуск - С.Г.Попов
Подписано к печати - 19.X.- 1992 г.
Формат бумаги 60x90 1/16 Объем 2,6 печ.л., 2,1 учетно-изд.л.
Тираж 220 экз. Бесплатно. Заказ N 76.

Ротапринт ИЯФ СО РАН , г. Новосибирск, 92